Performance Improvement of LFFC Schemes Base on B-Spline Networks for UPS Inverters

A. Rahmati [1] M. Taherkhani [2]

Abstract – Although Learning-based control method base on B-Spline Network (BSN) together with PD controller presents an excellent steady-state performance for Uninterruptible Power Supply (UPS) Inverters but it may not achieve high dynamic performance under non-periodic disturbances, which can be inappropriate for high performance UPSs. To further reduce the transient errors, in this paper a simple design and effective robust controller instead of PD controller is adopted parallel with the BSN. Simulation results under various conditions show that the proposed controller can achieve not only better dynamic performance but also can return better steady-state performance and further reduced THDs in the output voltage, compare to those of a BSN with PD scheme developed earlier.

Keywords – B-spline function, inverter, LFFC, robust controller, uninterruptible power supply.

I. INTRODUCTION

Uninterruptible Power Supply (UPS) systems supply emergency power in case of utility power failures and are widely used as backup power for critical loads such as computer and life support systems in hospitals. In UPS systems overall performance is dependent upon the static inverter- filter arrangement which is used to convert DC input power to high quality ac voltage of low Total Harmonic Distortion (THD). The performance of the system is measured both in terms of steady-state performance, such as voltage regulation and THD, and transient performance, such as response to a sudden change in load [1].

Many feedback control schemes have been proposed for UPS inverter, in order to achieve fast dynamic response and eliminate voltage distortions, which can occur under nonlinear loads.

Nonlinear loads that cause distortion in the output voltage are typically periodic, which suggests that learning-based control methods may have certain advantages over instantaneous-feedback control methods, such as deadbeat control and cascade control which are popular as high-performance controllers in the industry [2].

Learning-based control methods are considered for processes that repetitively perform a series of tasks [3]. During operation, such processes are subject to two types of disturbances; reproducible disturbances, those depend on the state of the process and hence reoccur each run in the same way, and remaining random disturbances. Generally learning-based control system has separate means for compensating both types of disturbances [3].

The paper first received 17 Sept 2009 and in revised form 9 June 2010.
Digital Ref: Digital Ref: A170801246

[1] Department of Electrical Engineering, Iran University of Science and Technology, E-mail: rahmati@iust.ac.ir

[2] Department of Electrical Engineering, Iran University of Science and Technology, E-mail: taherkhani@ee.iust.ac.ir

Random disturbances are compensated by a feedback controller. When random disturbances are small, this controller does not determine the performance of the controlled system. It can therefore be designed for robustness mainly, which does not require an accurate process model [3].

The reproducible disturbances are compensated by a feed-forward controller. Normally a feed-forward controller is designed on the basis of an accurate model of the process. To prevent the need of an accurate process model, the feed-forward controller is implemented as a neural network that is trained during control. The type of neural network that is used is a B-spline network (BSN) [3] which utilizes piecewise polynomial basis functions, known as B-splines or B-spline basis functions, to store information. Like other NNs, a BSN can approximate arbitrary continuous functions to any degree of accuracy as long as the network used is large enough. Unlike the global weight-updating scheme used in backpropagation-based NNs, the BSN operates with a local weight-updating scheme, with the advantages of fast convergence speed and low computational complexity. These features make it more suitable for providing real-time online solutions, as required in the present UPS inverter control, than the feedforward NNs with online backpropagation training [2]. This type of learning controller which use BSN as feedforward controller together with a fast feedback controller was introduced as the Learning Feed Forward Control (LFFC) scheme [3], [4]. Stability of LFFC is determined by the support of the B-splines and the value of the learning rate [2], [3], [4].

In previous research [2], a parallel feedback PD for compensating random disturbances and a B-spline network as the feed-forward controller for compensating reproducible disturbances was proposed for UPS inverter. It had been shown that overall controller system can achieve a very low THD and fast error convergence under different loads. But this paper acknowledges that the controller may not achieve high dynamic performance when the load is changed from no load to a non-linear cyclic load which can be inappropriate for high performance UPSs. Thus, this paper proposes a robust controller for improving the transient response of LFFC scheme with BSN under non-periodic disturbances. This paper is organized as follows: Section II describes the plant to be controlled and Section III shows the structure of the digital control system: BSN controller and robust controller. Section IV describes the design procedure of BSN with proposed robust controller. Section V presents some simulation results that show the transient and steady-state performance of the BSN with robust controller and compares it to those of the BSN with PD controller.

II. DYNAMIC MODEL OF A SINGLE PHASE UPS INVERTER

If the switching frequency of UPS inverter which is shown in Fig. 1 is high enough, its major dynamic response can be determined by just taking LC filter into account. Using circuit laws, the output voltage of the LC filter can be written as:

$$V_o(s) = \frac{r_C C s + 1}{LCs^2 + C(r_C + r_L)s + 1} U(s) - \frac{r_C CLs^2 + (L + r_C r_L C)s + r_L}{LCs^2 + C(r_C + r_L)s + 1} I_o(s) \quad (1)$$

Where U is the average input voltage of the filter, and I_o is the load current. By considering the load current as an external disturbance, the transfer function between output voltage and input voltage of the filter can be written as follows [2]:

$$G_p(s) = \frac{V_o(s)}{U(s)} = \frac{r_C C s + 1}{LCs^2 + C(r_C + r_L)s + 1} \quad (2)$$

In the z domain, the expression for the output voltage will have the form [2]:

$$V_o(k) = G_p(z)u(k) + di(k) \quad (3)$$

Here, $G_p(z)$ is the z transform of (2) with sampling period h. All cyclical disturbances that cause output voltage deviation (including distortion), such as the load current (linear and nonlinear loads) and the dead-time effect in the inverter switches, are summarized as di. The task of the BSN-based controller is to come up with a suitable control input $u(k)$ such that $V_o(k)$ tracks a sinusoidal reference in the face of the disturbance inputs $di(k)$ [2].

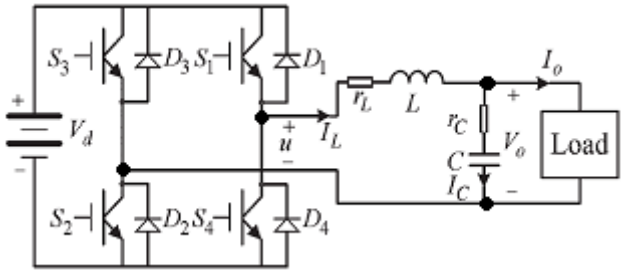

Fig. 1: Single-phase full-bridge inverter

III. LFFC CPNTROLSCHEME

The LFFC scheme with BSN controller together with the robust controller is shown in Fig. 2. During sampling interval k, the controller output may be written as:

$$u(k) = u_{ff}(k) + u_{fb}(k) + r(k) \quad (4)$$

Where u_{ff} and u_{fb} are the outputs of the feedforward BSN controller and the feedback robust controller, respectively, and r is the reference input to be tracked. The feedforward of r is used as the major component of the control effort to achieve better tracking [2].

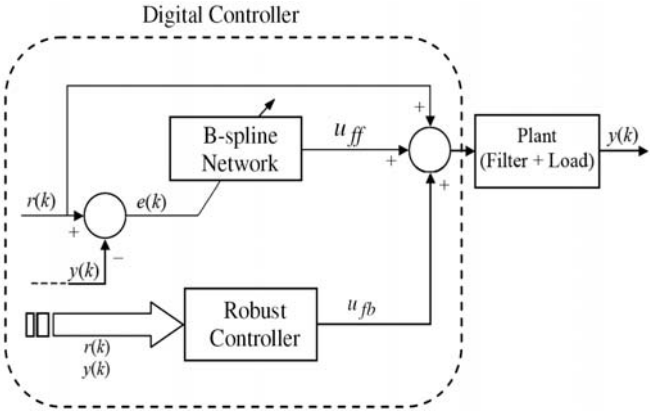

Fig. 2: Block diagram of the LFFC scheme with BSN and robust controller for UPS inverter system.

A. Robust controller

PID controllers' family is most popular controllers in industry because of good performance and simplicity in design. But the performance of these controllers is degraded tremendously when the system is exposed to disturbances or noise. H_∞ optimization method is a frequency domain approach for robust controller design and has been developed in response to the need for a synthesis procedure that explicitly addresses questions of modeling errors, unknown disturbances and noise. There are many ways in which feedback design problems can be cast as H_∞ optimization problems. A general formulation is afforded by the general configuration shown in Fig. 3 which is described by [5]:

$$\begin{bmatrix} z \\ \upsilon \end{bmatrix} = P(s)\begin{bmatrix} w \\ u \end{bmatrix} = \begin{bmatrix} P_{11}(s) & P_{12}(s) \\ P_{21}(s) & P_{22}(s) \end{bmatrix}\begin{bmatrix} w \\ u \end{bmatrix} \quad (5)$$

$$u = K(s)\upsilon$$

The signals are: u the control variables, υ the measured variables, w exogenous signals such as disturbances and commands, and z the so-called "error" signals which are to be minimized in some sense to meet the control objectives and P is the state-space realization of the generalized plant [5].

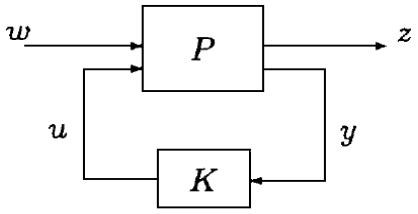

Fig. 3: General control configuration

The general control problem in this framework is to synthesize a controller that will keep the size of the performance variables z ,small in the presence of the exogenous signals, w .Hence, the disturbance rejection performance would depend on the "size of the closed-loop transfer function from w to z ,which we shall denote as $T_{zw}(s)$ .Thus, controllers are sought that minimize the "size" of the closed-loop transfer function $T_{zw}(s)$ .The two most common and physically meaningful norms that are used to classify the "size" of $T_{zw}(s)$ are the H_2 and H_∞ norms. As such, controllers are sought that minimize either the H_2 and H_∞ norm of [5].

$$T_{zw}(s) = \frac{Z(s)}{W(s)} = P_{11} + P_{12}K(1 - P_{22}K)^{-1}P_{21} = f_L(P, K) \quad (6)$$

This can be solved efficiently using the algorithm of Doyle et al. [6], [7]. It is not our intention to describe in detail the mathematical solutions, since efficient, commercial software for solving such problems is so easily available.

The signal based approach to controller design is very general and is appropriate for multivariable problems in which several objectives must be taken into account simultaneously. In this approach the class of external signals affecting the system and the norm of the error signals which must be keep small are defined. The focus of attention is the size of the error signals and away from the size and bandwidth of the close-loop transfer function.

A typical problem using the signal-based approach to H_∞ control is illustrated in the interconnection diagram of Fig. 4. The weights W_d , W_i , W_n may be constant or dynamic and describe the relative importance and/or frequency content of the disturbances, set points, and noise signals. The weights W_{ref} is a desired closed-loop transfer function between the weighted set point r_s and the actual output y. The weights W_e and W_u reflect the desired frequency content of error $y - y_d$ and the control signals u , respectively. The problem can be cast as a standard H_∞ optimization in the general control configuration by defining [6]:

$$w = \begin{bmatrix} d \\ r \\ n \end{bmatrix} \quad z = \begin{bmatrix} z_1 \\ z_2 \end{bmatrix} \quad v = \begin{bmatrix} r_s \\ y_m \end{bmatrix} \quad u = u \tag{7}$$

in the general setting of Fig. 4.

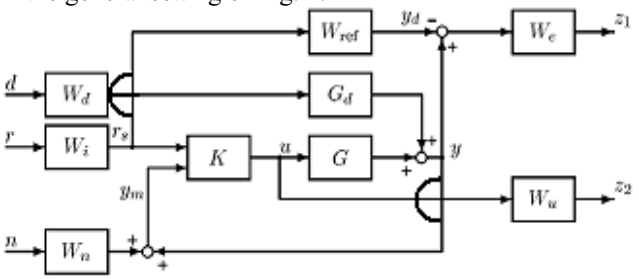

Fig. 4: A signal-based H_∞ control problem

B.BSN controller

A BSN utilizes piecewise polynomial basis functions, which are known as B-splines or B-spline basis functions, to store information. An n th-order B-spline consists of piecewise polynomial functions of order $(n-1)$ [2], [8] The function evaluation of a B-spline is generally called the membership and is denoted as μ (see Fig. 5). That part of the B-spline's input space for which μ is unequal to zero is called its support. Generally, the support of a basis function does not cover the whole input space. In addition, the supports overlap each other. When the supports overlap each other by more than 50%, the BSN is termed "dilated" [2], [8] .

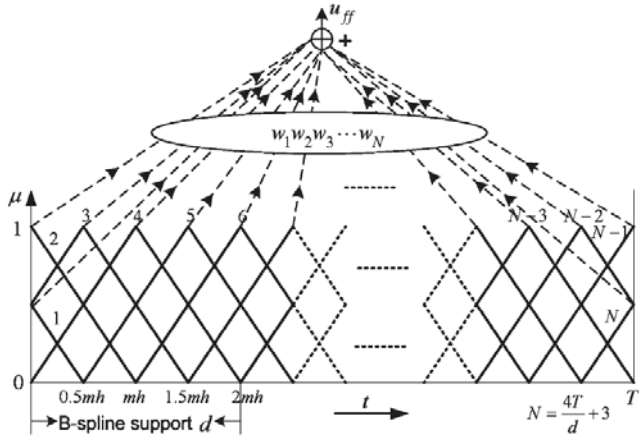

Fig. 5: B-spline network

BSN controller inherently has a low-pass feature that can be used to cut off learning at high frequencies and thereby ensure error convergence. Though a BSN with dilation 1 (50% overlap) can be very easy to implement and analyze, such a BSN did not provide large enough attenuation to cut off the learning at high frequencies. A BSN with dilation 2 (75% overlap) can be capable of satisfactorily meeting this requirement. Though BSNs with higher dilations can result in even better performance, they are much more complex to implement [2], [8].

The input of the feedforward BSN in Fig. 2 is simply the sampling sequence number k .Since the reference is periodic, the input space is $k \in [0, T/h]$, where the interval T is the fundamental period of the UPS inverter. To create an I/O mapping, the B-splines are placed on this domain of input variable, as shown in Fig. 5. The choice of a second order BSN resulted in the use of simple piecewise linear first order algebraic functions. Higher order B-splines are difficult to implement due to the resulting nonlinear functions [2].

The part of the input space for which $\mu_i(k)$ is not zero,i.e., the support of the B-spline, equals d . In one period T , if there be N equally spaced B-splines. Then, the B-spline support (or width) can be given by $d = 4T/(N-3)$. Moreover, with the total number of sampling points given by T/h , there will be $2m$ samples within one B-spline, where $m = d/2h$. The output of the BSN is a weighted sum of the B-spline evaluations, as shown in Fig. 5. Thus [2]:

$$u_{ff}^{j}(k) = \sum_{i} w_i^j \mu_i(k) \tag{8}$$

Where k is the index of sampling interval, j denotes the j th repetitive operation, w_i^j is the weight for B-spline i in iteration j , and $\mu_i(k)$ is the function evaluation, or membership, of the i th B-spline. From one fundamental cycle to the next one, the weight of the B-spline "i" in iteration j is updated by [2]:

$$w_i^j = (1-\alpha) w_i^{j-1} + \frac{\gamma \sum_{l=0}^{T/h} (\mu_i(l) er^{j-1}(l))}{\sum_{l=0}^{T/h} \mu_i(l)} \tag{9}$$

Where γ is the learning gain, α is the forgetting factor, and $er^{j-1}(l)$ is the tracking error of the previous iteration $(j-1)$. Though summation from $l=0$ to T/h is used in (9), the calculation is actually simple because $\mu_i(l) \neq 0$ only over the support interval of d . The forgetting factor α is introduced to increase the robustness of the BSN controller. Although, due to the forgetting factor, the tracking error will no longer converge to zero, the error can be made small enough for industrial applications. It has been verified in the experimental work that the introduction of the forgetting factor is necessary for the stable operation of the system [2].

As may be noted, the design of the BSN controller requires only two main parameters to be determined: 1) the B-spline support d and 2) the learning gain γ . The third parameter, namely, the forgetting factor α , is easily set by trial and error during the experimental stage or by experience [2].

From (8) and (9), it can be shown that the equivalent frequency-domain model of the BSN controller can be written as [2]**:**

$$u_{ff}^{j}(k) = (1-\alpha) u_{ff}^{j-1}(k) + 2\gamma H(\omega, a_k, d) er^{j-1}(k) \tag{10}$$

with [8]:

$$H(\omega,a_k,d)=\left(\frac{\sin(\omega d/4)}{\omega d/4}\right)^2[(1-a_k)e^{-j\omega(1+a_k)d/4}+a_k e^{j\omega(2-a_k)d/4}+(2-a_k)e^{-j\omega a_k d/4}+(1+a_k)e^{j\omega(1-a_k)d/4}]/2 \quad (11)$$

Equation (11) only models the controller in the frequency domain and does not represent its actual implementation. It may be noticed from (11) that for a given a_k, $H(\omega,a_k,d)$ is a function of the normalized frequency $x=\omega d/4$ [2]. The magnitude and phase plots of $H(\omega,a_k,d)$ for different a_k values are shown in Fig. 5 and 6.

Here, the a_k values are assumed to be constant, though they are not so in the actual case. The magnitude curves for different a_k values Fig. 5 are nearly identical and differ only very slightly. They have a notch at a value of x equal to π, i.e., at $x=\omega d/4=\pi$. This may also be seen from (11) in which $H(\omega,a_k,d)\to 0$ as $\omega d/4\to\pi$. At high frequencies, the phase shift curves with different a_k values do differ considerably. However, the phase shift is nearly zero prior to the notch point, even with different a_k values. Thus, at frequencies lower than $\omega_n=4\pi/d$, the time-varying nature of a_k does not affect the frequency response much and, hence, is conveniently ignored here [2], [9].

By applying the control law (8) and (9) and by assuming that the model of the inverter $G_p(z)$ has all the following features: 1) the desired output is repeated in each iteration; 2) the system starts with the same initial condition in each iteration; 3) the system dynamics is time invariant; and 4) the measurement noise of the output is negligible—it can be shown that [2]:

$$\begin{aligned}er^j(z)&=\frac{1-2\gamma H(\omega,a_k,d)P(z)+G(z)P(z)}{1+G(z)P(z)}er^{j-1}(z)\\&+\frac{\alpha P(z)u_{ff}^{j-1}(z)}{1+G(z)P(z)}\\&=(1-2\gamma H(\omega,a_k,d)G_C(z))er^{j-1}(z)\\&+\alpha G_C(z)u_{ff}^{j-1}(z)\end{aligned} \quad (12)$$

Here, $G_C(z)$ is the system transfer function with robust controller alone. With $z=e^{j\omega h}$ and (12), the stability requirement of the BSN controller is thus [2], [9]:

$$\left|1-2\gamma H(\omega,a_k,d)G_C(e^{j\omega h})\right|<1 \quad (13)$$

For all frequencies from zero to the Nyquist frequency. To ensure rapid error convergence, the error decay factor, which is defined as $\left|1-2\gamma H(\omega,a_k,d)G_C(e^{j\omega h})\right|$, should be made small [2].

IV. LFFC Control Design

The parameters of the inverter system for the design are shown in Table I. As a first design step, the robust controller, used with the BSN was designed.

A.Robust controller design

The objective of robust controller design is reducing the effect of the I_o as disturbance on the system. Thus we considered following expressions for H_∞ optimization problem:

$$w=\begin{bmatrix}i_o\\r\end{bmatrix}\quad z=\begin{bmatrix}W_e(r-v_o)\\W_u u\end{bmatrix}\quad v=\begin{bmatrix}r_s\\v_o\end{bmatrix}\quad u=u \quad (14)$$

$$P=\begin{bmatrix}G_d & -1 & G_p\\0 & 0 & 1\\G_d & 0 & G_p\\0 & 1 & 0\end{bmatrix}$$

Where G_d represent the effects of load current on output voltage which is second term of (1) as follows:

$$G_d(s)=-\frac{r_C CLs^2+(L+r_C r_L C)+r_L}{LCs^2+C(r_C+r_L)s+1} \quad (15)$$

The frequency of the major components of a typical nonlinear load current waveform are below 550 Hz [10]; hence, the major components of the tracking error will also be below 550 Hz therefore W_e was selected as a low pass filter with 550Hz cutoff frequency whereas W_u was selected a constant less than 1 for ensuring that the control signal will not be too large.

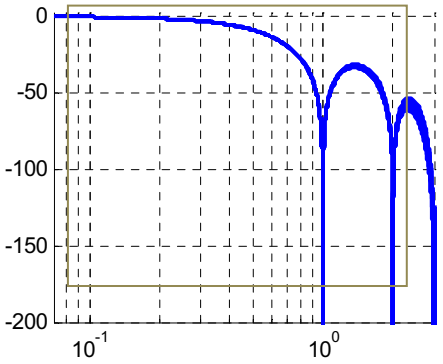

Fig. 5: Magnitude plot of $H(\omega,a_k,d)$ —plotted assuming constant a_k values

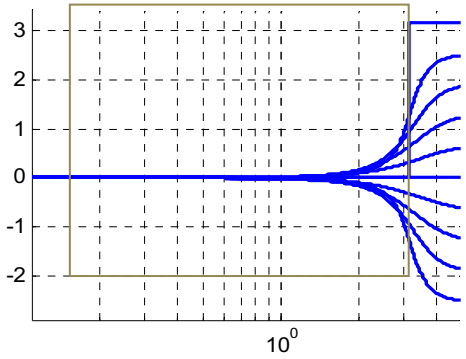

Fig. 6: Phase plot of $H(\omega,a_k,d)$ —plotted assuming constant a_k values

Table I: Inverter parameters

Parameter	Value
Filter inductor	0.58mH
Filter capacitor	117.1μF
Sampling frequency	10kHz
Switching frequency	10kHz
DC link voltage	150V
Reference voltage	100V,50Hz
Inductor resistance	0.065Ω
Capacitor resistance	0.07Ω
Rating power	1kVA

Given this representation of the design goals, and using MATLAB the proposed robust controller will be a transfer function of order 3 such that the control signal is as follows:

$$U(z)=\left(\frac{-496.3z^2+473.4z-1.583\times10^{-5}}{z^3-1.367z^2+0.4266}\right)V_o(z)+\left(\frac{2009z^2-3590z+1603}{z^3-1.367z^2+0.4266}\right)V_{ref}(z) \quad (16)$$

For comparison, the PD control signal which was designed by step-response method for this inverter in [2] was:

$$U(z)=\left(2.04+0.5453\frac{3(z^2-1)}{z^2+0.5359z+0.0718}\right)V_o(z)-\left(2.04+0.5453\frac{3(z^2-1)}{z^2+0.5359z+0.0718}\right)V_{ref}(z) \quad (17)$$

Fig. 7 shows step response of close loop system with PD and robust controller. It is obvious that robust controller has improved system transient response noticeably. Moreover it presents a better steady-state performance than PD controller as can be seen from Fig. 7.

Fig. 8 presents the bode diagram of output voltage versus load current i_L when frequency is below 3768 rad/sec (600 Hz). It can be seen that output voltage with robust controller has been less impressible from load current compare to PD controller, on the other hand robust controller can reduce the effects of i_L as an external disturbance on the inverter output voltage better than PD controller. (As mentioned before the major components of a typical nonlinear load current waveform are below 550Hz; hence considering frequency range of this diagram below 600Hz can be adequate.)

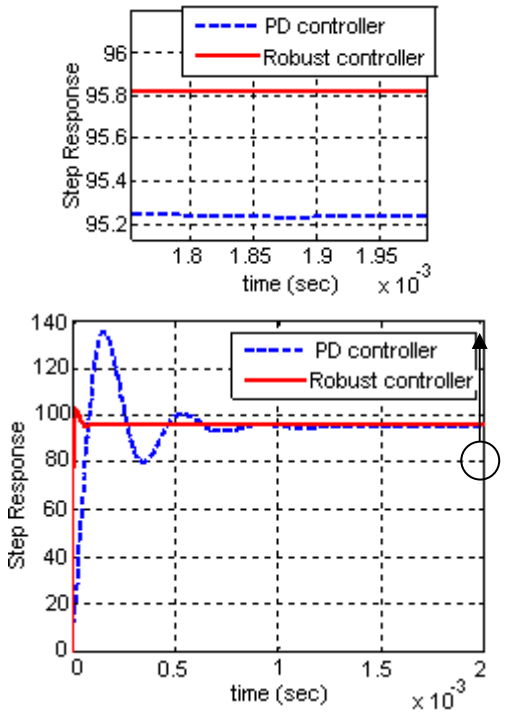

Fig. 7: Close loop system with PD and robust controller step response

B. BSN controller design

For BSN controller design, BSN parameters: the B-spline support d and learning gain γ must be determined.

Choice of BSN support d: As mentioned before, for the stability requirement, (13) must be satisfied for all frequencies up to the Nyquist frequency. From the closed-loop response $G_C(e^{j\omega h})$ with robust controller, as shown in Fig. 9 we can see that magnitude and phase plots of $G_C(e^{j\omega h})$ is approximately constant up to the Nyquist frequency (31416rad/sec or 5kHz) thus (13) is satisfied if we select $H(\omega,a_k,d)$ notch frequency bellow Nyquist frequency:

$$\omega_n=4\pi/d<31416\Rightarrow d>0.0004 \quad (18)$$

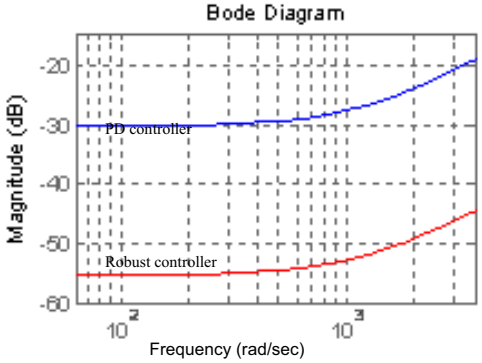

Fig. 8: Bode diagram of output voltage (vo) versus load current (i_L)

since the major components of the tracking error will also be below 550 Hz. Therefore, the notch frequency $f_n=2\pi/\omega_n$ must be kept higher than 550 Hz, or d must be kept less than $1/275=0.0036$ [2]. Thus the design range for d is:

$$0.0004<d<0.0036 \quad (19)$$

d was set at 0.002.

Choice of Learning Gain γ: With a small γ value, though the error convergence requirement in (13) will always be satisfied, the speed of error convergence will be slow. On the other hand, with too large a learning gain, the error convergence requirement in (13) may not be satisfied. At low frequencies, $G_C(e^{j\omega h})$ has almost constant gain (e.g., A_G).Thus, if γ is selected such that [2]:

$$\gamma=\frac{1}{2A_G} \quad (20)$$

Then the error decay factor will be nearly zero up to Nyquist frequency, and very fast error decay can be expected [2]. From the closed-loop response $G_C(e^{j\omega h})$, as shown in Fig. 9, the values of A_G is 0.25 thus According to (20), $\gamma=2$ and a forgetting factor $\alpha=0.01$ was used for the BSN controller.

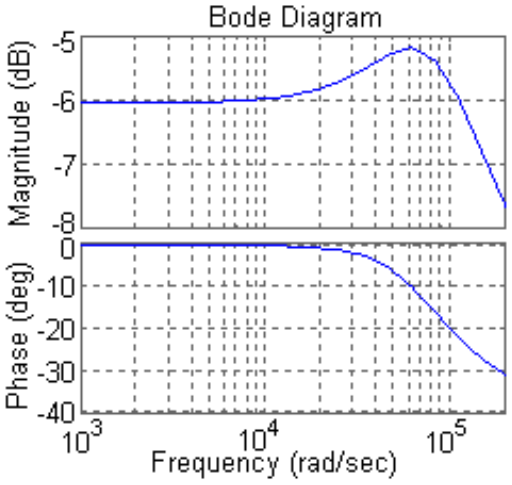

Fig. 9: Bode plots of close loop system with robust controller

V. Simulation Results

Fig. 10 shows the transient performance with PD controller and Fig. 11 with robust controller when the load is changed from no load to a rectifier load in a step fashion in both cases. It can be seen that the transient errors caused by nonlinear cyclic load are significantly reduced when the roust controller is used as feedback controller instead of PD controller. Whereas with PD controller maximum peak of transient tracking error is exceeded from 15V, with robust controller is less than maximum value of steady state error (4V).

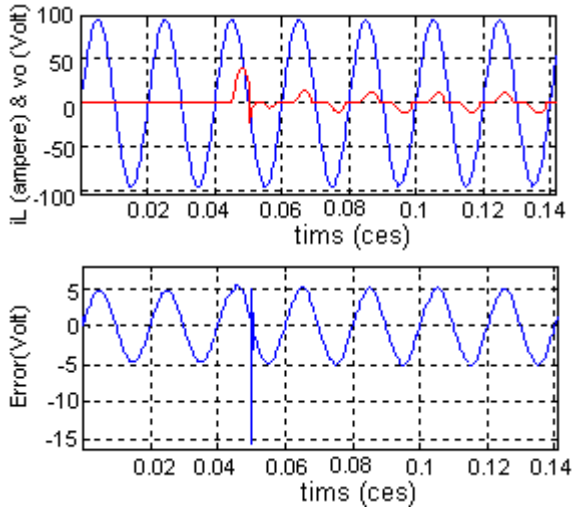

Fig. 10: Transient response waveforms when the load changes from no load to a rectifier load—system with PD controller.

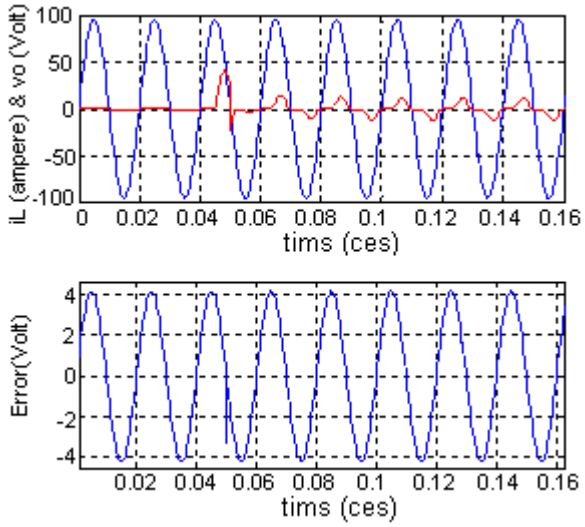

Fig. 11: Transient response waveforms when the load changes from no load to a rectifier load—system with robust controller.

Fig. 12 shows the steady-state output voltage and the load current and output voltage error waveforms of the inverter for a nonlinear load (crest factor = 3) with the BSN and PD controller. THD of the output voltage is 0.7% and The fundamental peak value of the output voltage is 97.94 V, with a reference voltage of 100 V. Fig. 13 shows the steady-state output voltage and the load current and output voltage error waveforms of the inverter for a nonlinear load (crest factor = 3) with the BSN and robust controller. It is notable that harmonics in output voltage in this case were enough small such that there was not any measurable value for THD in simulation result and fundamental peak value of the output voltage was 99.5 V, with a reference voltage of 100 V. Fig. 14 compares tracking error in both cases with more detail and more extended time range. Thus we can see that robust controller has improved not only transient performance but also has returned better steady-state performance and has reduced output voltage THD tremendously.

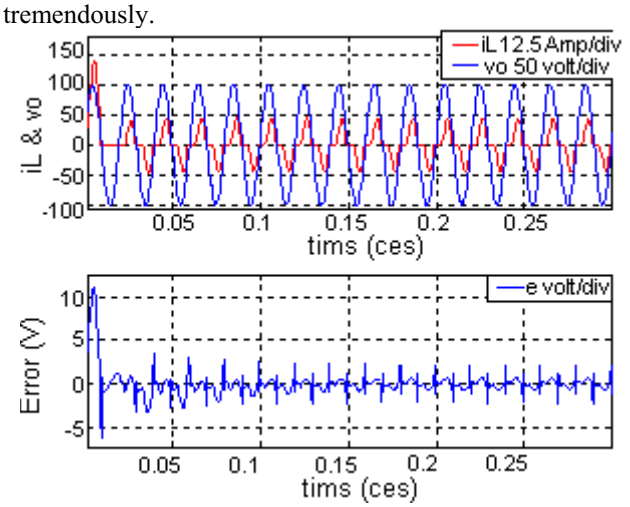

Fig. 12: Output voltage, current waveforms and output voltage tracking error with a nonlinear load—BSN with PD controller.

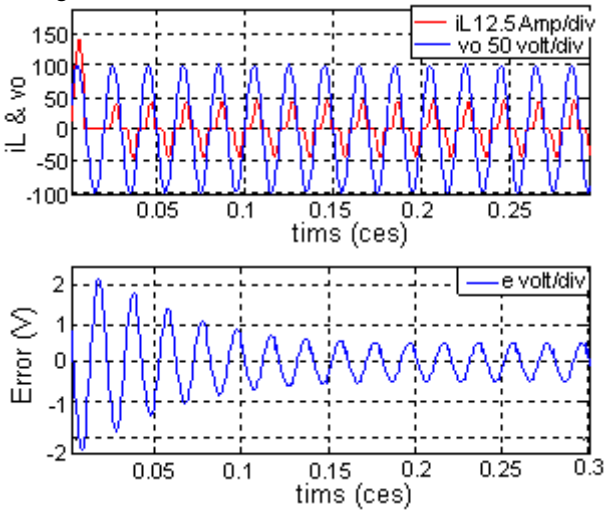

Fig. 13: Output voltage, current waveforms and output voltage tracking error with a nonlinear load—BSN with robust controller.

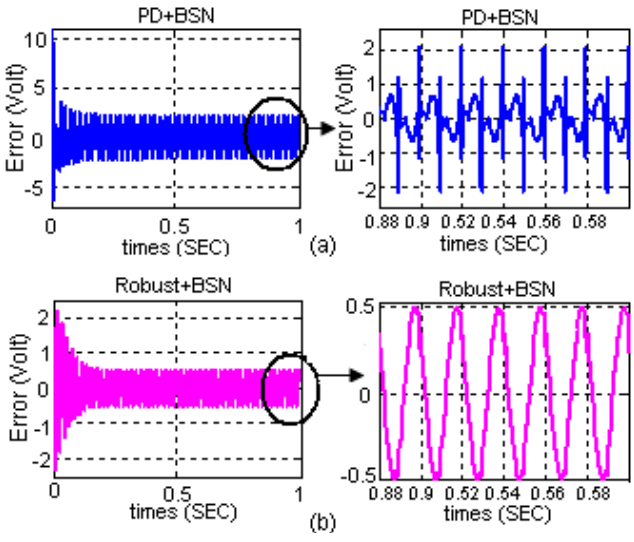

Fig. 14: Output voltage tracking error with a nonlinear load. (a) BSN with PD controller (b) BSN with robust controller

VI. CONCLUSION

Although LFFC Schemes with B-Spline Networks and PD controller have led to very good steady state performance for single phase inverter UPSs but their transient response under non-periodic disturbances may not be suitable for high performance UPSs. Therefore, this paper proposed a more sophisticated controller as feedback controller for compensating transient errors. Simulation results showed that the robust controller with a fix structure and simple design can minimize non-periodic disturbances caused by nonlinear cyclic loads and unmodeled dynamics. Moreover the proposed controller together with BSN controller showed better steady-state performance and output voltage THDs compare to those of PD with BSN controller.

REFRENCES

[1] H. Deng, R. Oruganti and D. Srinivasan, "Digital control of single-phase inverters with modified PWMtechnique", in Proc. IEEE PESC, Jun. 2004, pp. 1365–1371.

[2] H. Deng, R. Oruganti and D. Srinivasan, "Neural Controller for UPS Inverters Based on B-Spline Network", IEEE Trans. Ind. Electron, vol. 55, no. 2, Feb. 2008

[3] W. J. R. Velthuis, T. J. A. de Vries and E. Gaal, "Experimental verification of the stability analysis of learning feed-forward control", in Proc. 37th IEEE Conf. Decision Control, Tampa, FL, 1998, pp. 1225–1229.

[4] W. J. R. Velthuis, "Learning feed-forward control—Theory, design and applications", Ph.D. dissertation, Univ. Twente, Enschede, The Netherlands, 2000.

[5] Leonard Lublin. Simon Grocott and Michael Arhans, The Control Handbook, CRC Press in Cooperation with IEEE Press, 1999, pp. 651-663.

[6] Sigurd Skogestad, Ian Postlethwaiye, Multivariable Feedback Control Analysis and Design, John Wiley & Sons, 1999, pp. 371–420.

[7] J. C. Doyle, K.Glover, P. P. Khargonekar and B. A. Francis, "state-space solutions to standard and control problems", IEEE Transactions on Automatic Control. 34(8): 831-847

[8] M. Brown and C. Harris, "Neurofuzzy Adaptive Modeling and Control", Englewood Cliffs, NJ: Prentice-Hall, 1994.

[9] Y.Q. Chen, K. L. Moore and V. Bahl, "Learning feedforward control using a dilated B-spline network: Frequency domain analysis and design", IEEE Trans. Neural Netw, Vol. 15, No. 2, Mar. 2004, pp. 355–366.

[10] J. Kim, J. Choi and H. Hong, "Output LC filter design of voltage source inverter considering the performance of controller," in Proc. PowerCon, Dec. 2000, Vol. 3, pp. 1659–1664

BIOGRAPHIES

Abdolreza Rahmati was born in Abadeh, Iran, in 1951. He received the B.Sc. degree in electronics engineering from Iran University of Science and Technology (IUST), Tehran in 1979, and the M.Sc. and Ph.D. degrees in power electronics from Bradford University, West Yorkshire, U.K. in 1987 and 1990, respectively. He has been a member of the faculty at IUST where he is currently an Associate Professor. He was Deputy for Educational Affairs and Postgraduate Studies in the Department (1992 to 2003), and a Visiting Professor at the Illinois Institute of Technology (IIT), Chicago (September 2004 to May 2005). His fields of interest are microprocessors and microcontroller-based system design, motor drives and control, HVDC transmissions, modulation strategies for power electronic systems, multilevel inverters, and power devices. Dr. Rahmati is a member of the Institution of Engineering and Technology (IET), Engineering Council, U.K.

Masoomeh Taherkhani was born in Takestan, Iran, in 1983. She received the M.Sc. degree in electronics engineering in 2009 and she is currently pursuing the PH.D at Iran University of Science and Technology (IUST), Tehran, Iran. Her research interest is in artificial intelligence in control and power electronics.